



## Impact of Gill Parasites on Biochemical Parameters in *Scomberomorus commerson* Fish

Walaa A. El-Shaer<sup>1</sup>, Samah A. Abdel-Hafiz<sup>2</sup>, Asmaa M. I. Abuzeid<sup>3\*</sup>

<sup>1</sup>Fish Diseases Unit, Animal Health Research Institute, Ismailia branch, Agriculture Research Center (ARC), Giza 12618, Egypt

<sup>2</sup>Biochemistry Unit, Animal Health Research Institute, Ismailia branch, Agriculture Research Center (ARC), Giza 12618, Egypt

<sup>3</sup>Department of Parasitology, Faculty of Veterinary Medicine, Suez Canal University, Ismailia 41522, Egypt

\*Corresponding Author: [asmaa\\_ibrahim@vet.suez.edu.eg](mailto:asmaa_ibrahim@vet.suez.edu.eg)

### ARTICLE INFO

#### Article History:

Received: Feb. 2<sup>nd</sup>, 2025

Accepted: March 15, 2025

Online: March 30, 2025

#### Keywords:

Gill parasites,  
*Scomberomorus commerson*,  
Prevalence,  
PCR,  
Phylogeny,  
Antioxidant response,  
Liver enzymes

### ABSTRACT

Gill parasites cause mass mortalities and significant economic losses in the fish industry. This study aimed to identify gill parasites infesting *Scomberomorus commerson* fish based on morpho-molecular tools and to evaluate their effects on biochemical indices and oxidative stress markers in fish. Eighty fish samples were collected from the Suez Canal in Ismailia Province, Egypt. Mixed parasitic infestation was recorded in 48.7% of fish, comprising *Livoneca redmanii* isopods and three monogeneans, *Cathucotyle cathuauui*, *Pricea multae*, and *Pseudothoracocotyla ovalis*. *Pricea multae* had the highest prevalence (67.5%) and intensity (29-80 parasites/fish). This study provided a new occurrence of *C. cathuauui* and *P. ovalis* from Egypt. The first mitochondrial cytochrome oxidase subunit 1 (*cox1*) data were reported from the three monogenean species. The two *C. cathuauui cox1* sequences were highly homologous and aggregated in a well-supported node in the phylogenetic trees, confirming the morphological identification. The genetic differences and phylogenetic links between *P. multae* and *P. ovalis* did not support the Thoracocotylidae family classification. Infested fish showed atrophy, degeneration, marbling appearance, and paleness of gills with excessive mucus secretion. Lactate dehydrogenase, aspartate aminotransferase, and alkaline phosphatase activities were significantly higher in heavily and moderately infested fish compared to the control group. Alanine aminotransferase levels showed a significant increase in the heavily infested group. Superoxide dismutase and catalase activities significantly decreased in the heavily infested group. Results suggest that the *cox1* gene is a valuable marker for identifying monogeneans, and call for controlling gill parasites.

### INTRODUCTION

Fish are a vital source of income due to their substantial economic value. Various species of marine fish, particularly those in the Scombridae family, are known for their high value and migratory nature. The narrow-barred Spanish mackerel (*Scomberomorus*

*commerson*, Lacépède, 1800, Family Scombridae) is a predatory marine fish prized for its rich, nutrient-dense proteins, making it one of the most expensive and high-quality fish (Thai *et al.*, 2021). *Scomberomorus commerson* spreads in the Indian and Pacific oceans, including the Red Sea and the Persian Gulf (Di Natale *et al.*, 2009; Abd EL Maged *et al.*, 2024). This migratory fish species has crossed the Suez Canal to the eastern Mediterranean Sea (Di Natale *et al.*, 2020). In Egypt, fishing methods, such as purse seines, gillnets, and rod-and-reels, have long been employed to capture this important and highly valuable epipelagic fish species (Abd EL Maged *et al.*, 2024). The gills of mackerels are a common habitat for ectoparasites (El-lamie *et al.*, 2022; Rothman *et al.*, 2022; Abd EL Maged *et al.*, 2024). Monogeneans are among the most common fish ectoparasites, usually attached to the host's skin and gills. Monogeneans are hazardous organisms that limit aquaculture productivity since they often coexist with other parasites or secondary bacterial infections (Silva *et al.*, 1997; Assane *et al.*, 2022; Yıldırım *et al.*, 2024). These parasites caused mass mortalities and many epidemics (Lia *et al.*, 2007) and can lead to commercial fish losses in both developed and emerging nations (Tessema, 2020). Cymothoid isopods are protandric hermaphrodites that inhabit the host's buccal and gill cavities and thrive on the blood, mucus, and flesh of several freshwater, marine, and estuarine fish species (Zayed *et al.*, 2023). Cymothoid isopods induced atrophy, bleeding at the connection site, and a slight protrusion of the gill cover (Rashed *et al.*, 2021). These ectoparasite infestations cause economic losses to the fish industry because they not only cause direct harm to fish but also disfigure them, making ornamental and food-grown fish unfit for sale (Tsfay *et al.*, 2024). Thus, the identification and control of these ectoparasites are essential.

The identification of ectoparasites typically depends on morphological characteristics. The two main monogenean groups (Monopisthocotylea and Polyopisthocotylea) are distinguished according to the structure of a well-developed adhesive attachment organ called haptor. The posterior haptor (opisthaptor) carries clamps or suckers in Polyopisthocotylea (Hayward, 2005) and one or two pairs of anchors (hooks) in Monopisthocotylea (El-lamie *et al.*, 2022). Compared to morphological methods, molecular markers provide a quicker and more efficient tool for the identification and phylogenetic investigation. The mitochondrial *cox1* gene, 18S ribosomal RNA gene, the 28S rRNA gene, and the internal transcribed spacers of rDNA (ITS) are the most frequently used markers for identifying monogenean species and studying their evolution and phylogenetic relationship (Shi *et al.*, 2014; Lewisch *et al.*, 2021; Baghdadi *et al.*, 2022; El-lamie *et al.*, 2022; Rothman *et al.*, 2022). Previous studies have used the 28S rRNA gene to identify some monogenean parasites (*Pricea multae*, *Cathucotyle cathuau*, *Pseudothoracocotyla ovalis*) from *S. commerson* (Baghdadi *et al.*, 2022; Rothman *et al.*, 2022). Although mitochondrial DNA evolves more rapidly than nuclear DNA and is a potent and valuable genetic marker in uncovering species-level phylogeny (Thaenkham *et al.*, 2022), the mitochondrial *cox1* gene has not been recovered from these species.

Parasitic infestations in the gills often lead to significant physiological and biochemical disruptions, triggering various bodily responses. These responses include circulatory abnormalities, proliferative and inflammatory reactions, and degenerative changes. Common manifestations include congestion, telangiectasia (dilation of small blood vessels), hemorrhages, and edema. Additionally, such infestations can cause epithelial hyperplasia, a rise in mucous cell production, inflammation, and tissue necrosis (Cantanhêde *et al.*, 2018). Oxidative stress plays a significant role in the progression and dynamics of parasitic infections, affecting both the infected host and the parasite as it adapts to survive within the host environment (Çenesiz, 2020; Szewczyk-Golec *et al.*, 2021). Moreover, the parasite develops complex defense strategies and builds resistance to the effects of reactive oxygen species (ROS) to ensure its survival within the host organism (Szewczyk-Golec *et al.*, 2021). This adaptation involves using available resources and the host's environment to support the parasite's growth while weakening the host. Reactive oxygen species (ROS) are crucial in defending against parasitic and microbial invasions (Dickson & Zhou, 2020). The host leverages the damaging effects of reactive oxygen species (ROS) on the parasite's cells to eliminate it. In response to an invading pathogen, phagocytic cells, such as granulocytes, monocytes, and macrophages, trigger a significant increase in oxygen consumption, often referred to as the "oxygen burst" or "respiratory burst," to combat the infection (Sorci & Faivre, 2009). This reaction generates and releases large amounts of superoxide anion and hydrogen peroxide (H<sub>2</sub>O<sub>2</sub>) to fight bacterial, viral, and parasitic infections (Maldonado *et al.*, 2020). Goldfish parasitized by the gill monogenean *Dactylogyrus* sp. exhibited more severe oxidative stress and lipid peroxidation compared to non-parasitized individuals (Mozhdeganloo & Heidarpour, 2014). However, no data revealed biochemical alterations in *S. commerson* infested with gill parasites. The current study aimed to identify the common gill parasites in *S. commerson* based on morphological and molecular characteristics and to determine serum biochemical changes associated with this infestation.

## MATERIALS AND METHODS

### 1. Fish sampling

Eighty fish samples of wild marine *Scomberomorus commerson* were randomly collected from the Suez Canal in Ismailia City, Egypt, between May and November 2024. The fish were promptly transported to the laboratory at the Ismailia branch of the Animal Health Research Institute. The collected specimens ranged from 35 to 42cm long and weighed between 450 and 650 grams.

## 2. Clinical and post-mortem examination of fish

External and internal inspections of living and freshly dead fish were performed based on the method of **Conroy and Herman (1970)** to identify any abnormalities.

## 3. Parasitological examination

Fish body surface, buccal cavity, gills, and branchial chamber were macroscopically and microscopically inspected for detecting parasites according to **Aneesh *et al.* (2014)**.

## 4. Morphological identification of parasitic samples

The collected isopods were washed in a warm saline solution before being examined under a dissecting stereomicroscope and light microscopy, and then immediately preserved in 70% ethyl alcohol. The total length of the isopods was measured and recorded in millimeters. Isopod morphological traits were described and identified following **Brusca (1981)**. The isolated monogeneans were fixed in 3% formalin, stained with Semichon's acetocarmine, rinsed several times with distilled water, dehydrated in a 70-100% ethanol series, cleared in clove oil and then xylene, and mounted in Canada balsam. Parasite images were gained with a Leica DM1000 microscope before processing by the ImageJ software (LOCI, University of California, Irvine) to measure the monogenean species. Measurements of adult monogeneans were obtained by analyzing five specimens/species and are presented as minimum to maximum (mean  $\pm$  SE).

## 5. Molecular identification of monogenean species

### 5.1. DNA extraction

The total genomic DNA was extracted from adult monogenean specimens (3-6 for each species) stored at  $-20^{\circ}\text{C}$  following the manufacturer's protocol of the Thermo Scientific™ Genomic DNA Purification Kit (Cat. No. K0512, Thermo Fisher Scientific, Waltham, MA, USA). A NanoDrop ND-1000 spectrophotometer (Thermo Fisher Scientific, Waltham, MA, USA) was used to measure the DNA concentration and determine the DNA amount incorporated in PCR reactions. The isolated DNA samples were preserved at  $-20^{\circ}\text{C}$ .

### 5.2. Amplification of the *mt-cox1* sequences

PCR amplification of the *mt-cox1* sequence was accomplished using universal MCOX1F2 (5'-TTTGGYCA YCCAGARGTGTA-3') and MCOX1R3 (5'-ACACGWC GTGGTAAACCACA-3') primers (**Zhang *et al.*, 2012**). The primers were manufactured in FASMAC Co. Ltd. (Atsugi, Japan). The PCR reactions (25 $\mu$ L) comprised EmeraldAmp MAX Master Mix (12.5 $\mu$ L, Cat. No. RR320A, Takara Bio,

Kusatsu, Japan), 1 $\mu$ L of each forward and reverse primer (10pmol/  $\mu$ L), template DNA (50ng), and ddH<sub>2</sub>O (up to 25 $\mu$ L). SensoQuest Labcycler 48 (SensoQuest GmbH company, Germany) was used to run the PCR program as follows: 98°C for 1min; 30 cycles of 98°C for 10s, 45°C for 30s, and 72°C for 2min; and 72°C for 5min. The amplified PCR products were examined by 1% ethidium bromide-agarose gel electrophoresis. The QIAquick PCR Purification Kit (Cat. No. 28104, Qiagen, Hilden, Germany) was used for cleaning PCR products before applying them for sequencing in both directions on the Applied Biosystems 3130 automated DNA sequencer (Applied Biosystems, Foster, CA, USA) with a ready reaction BigDye Terminator V3.1 cycle sequencing kit (Cat. No. 4336817, Applied Biosystems, Foster, CA, USA).

### 5.3. Bioinformatic analysis

We used the Basic Local Alignment Search Tool (BLAST) on NCBI to identify homologous sequences and selected 24 sequences for the phylogenetic analysis, including *Diplorchis hangzhouensis cox1* sequence (JQ038227.1) as an outgroup. The fragments were aligned using the MAFFT tool (Katoh *et al.*, 2017) under the L-INS-i algorithm. The pairwise distance in MEGA X was analyzed using the method of Kumar *et al.* (2018b). The alignments were manually curated in MEGA X to eliminate the poorly aligned regions where the final dataset incorporated in the phylogenetic analysis contained 588 positions. MEGA X was used to predict the best-fitting nucleotide substitution model for the maximum likelihood (ML) phylogeny depending on the AIC (Akaike Information Criterion). Meanwhile, the best-fitting model for Bayesian inference (BI) phylogeny was predicted by MrModeltest2-v.2.4. GTR + I + G model was applied in both analyses. The ML phylogenetic tree was reconstructed in MEGA X, and bootstrap values from 1000 resampled datasets were used to evaluate the nodal support. The BI analysis was conducted in MrBayes v. 3.2.1 with Markov chain Monte Carlo (MCMC) chains run for 1,000,000 generations with a 100 sample frequency. After plotting the log-likelihood scores, the first 25% of samples were eliminated from the cold chain (burnfrac=0.25). FigTree v.1.4.3 was utilized to visualize the ML and BI phylogenetic trees.

## 6. Blood biochemistry

### 6.1. Blood sampling

For biochemical analysis, we prepared three groups, each containing five individuals. Group 1 represented control parasite-free fish. Fish infested with monogeneans denoted Group 2, while Group 3 contained fish with mixed isopod and monogenean infestations. Blood was collected from the examined fish by cardiac puncturing using sterile disposable plastic syringe with 22-gauge needle. The collected blood samples, which were not heparinized, were centrifuged at 3000 rpm for 5 minutes.

The resulting serum was separated and stored at  $-18^{\circ}\text{C}$  for subsequent analysis (Svobodová & Vykusová, 1991).

### 6.2. Lactate dehydrogenase enzyme assay

The fish blood serum was used to estimate lactate dehydrogenase enzyme (LDH) by using the method of Cabaud and Wroblewski (1958).

### 6.3. Liver function tests

Alanine aminotransferase and aspartate aminotransferase (AST) were assayed by the method of Huang *et al.* (2006). Alkaline phosphatase (ALP) activity was estimated according to the method of Estiarte *et al.* (2007).

### 6.4. Oxidative stress markers

Superoxide dismutase (SOD) activity was analyzed following Nishikimi *et al.* (1972). The catalase (CAT) activity and MDA level were determined according to Aebi (1984) and Bird and Draper (1984), respectively.

## 7. Statistical analysis

The data were analyzed using the one-way ANOVA in the SPSS version 19 (SPSS Inc., Chicago, IL, USA) statistical package. The difference between groups were evaluated by Duncan's post-hoc test. A statistical significance was considered at a *P*-value less than 0.05.

## RESULTS

### 1. Clinical and post-mortem findings of infested fish

The fish naturally infested with Cymothoid isopods and monogeneans were hypoxic and showed a noticeable unilateral or bilateral elevation of the fish's gill cover, with paleness of gill filaments (Fig. 1A). Mixed isopod-monogenean infestation was also accompanied by degeneration, necrosis, atrophy, marbling appearance, and detachment of gill filaments, and excessive mucus secretion (Fig. 1B). When removing isopods, it was firmly attached to gill filaments (Fig. 1C) leaving pits and tissue destruction at the site of attachment (Fig. 1D & E). A gravid female isopod deposits eggs in a brood clutch (marsupium) molting to mancae, which were occasionally seen (Fig. 1F). Fish infested with monogeneans demonstrated paleness and degeneration of gill filaments (Fig. 1G). Fig. (1H) shows different monogenean species collected from gills.

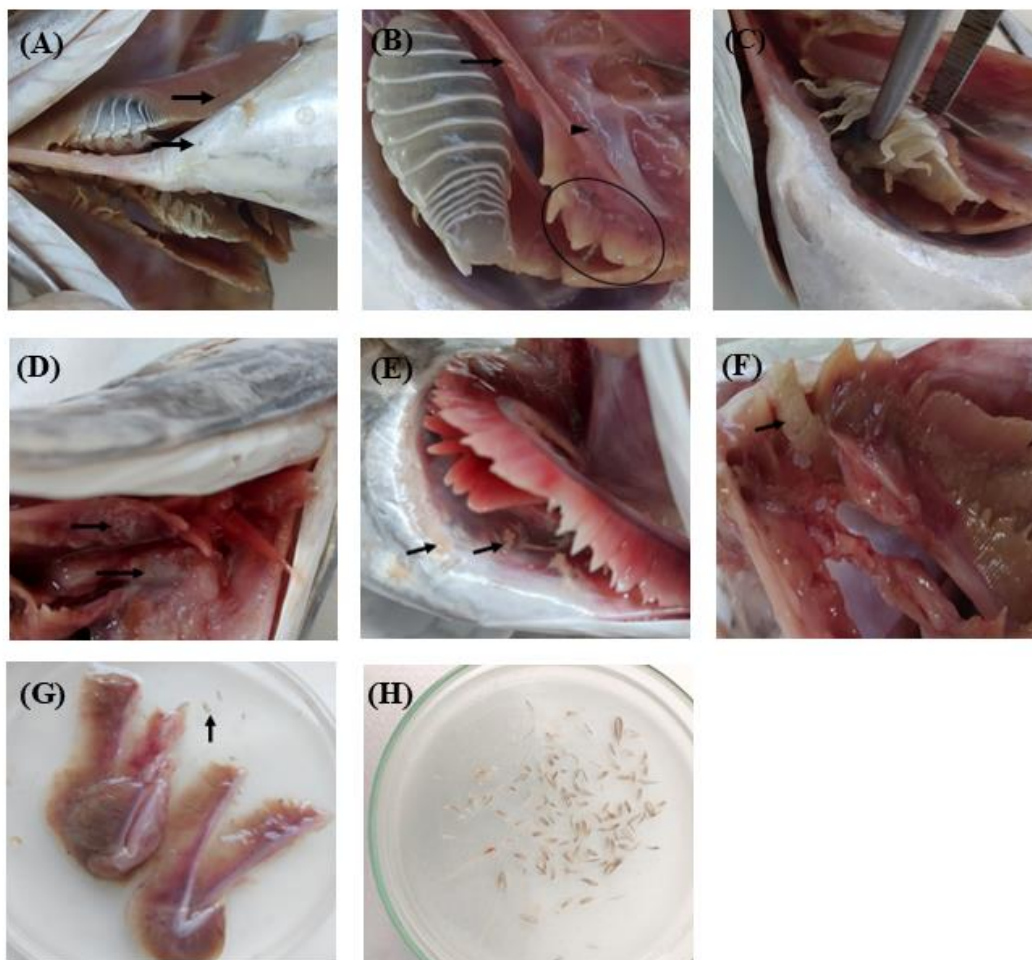


**Fig. 1.** Post-mortem picture of naturally infested *Scomberomorus commerson*. (A) Paleness of gills and bilateral elevation of operculum due to isopod infestation mixed with monogenean infestations (black arrows), (B) Mixed isopod and monogenean (black circle) infestations associated with degeneration, atrophy, and detachment of the gill filaments (black arrow) and excessive mucus secretion (arrowhead), (C) Firmly attached adult isopod to gill filaments, (D) Tissue damage and necrosis at the site of isopod attachment (black arrows), (E) Pits (black arrows) left after removal of isopods, (F) The isopod manca (black arrow) attached to fish gills, (G) Paleness and degeneration of gill filaments accompanying monogenean (black arrow) infestation, (H) Different species of monogenean parasites isolated from gills.

## 2. Prevalence and intensity of parasites

A total of 48.7% of the examined fish samples revealed *Livoneca redmanii* uni or bilateral gill infestation (intensity 1-3/fish) accompanied by monogenean infestation (49.7% mixed isopod-monogenean infestation). Monogenean gill parasites were present in 67% of examined *S. commerson*. Three gill-infesting monogenean species (*Pricea multae*, *Cathucotyle cathuau*, and *Pseudothoracocotyla ovalis*) were recorded with a

prevalence of 67.5, 62.5, and 37.5%, respectively. The most abundant monogenean parasite was *P. multae*, with an infestation intensity ranging from 29 to 80 parasites per fish, while the least abundant monogenean was *P. ovalis* (1-13 per fish) (Table 1).

**Table 1.** Prevalence and intensity of parasitic infestation among examined fish

Fish (n= 80)	Mixed infestation	Isopod ( <i>Livoneca redmanii</i> )	Total Mon.	<i>Cathucotyle cathuaui</i>	Monogenea	
					<i>Pricea multae</i>	<i>Pseudothoracocotyla ovalis</i>
No. of infested fish	39	39	54	50	54	30
Prevalence %	48.7	48.7	67.5	62.5	67.5	37.5
Intensity (parasites/fish)		1-3	46-123	12-30	29-80	1-13

Mon., Monogenea.

### 3. Morphological description of isolated parasites

#### *Livoneca redmanii* Leach, 1818

The total body length of the female is 1.2-2.4cm, and the maximum width is 1.2-1.4cm. Adults have an oval body that is sometimes twisted on one side. The body comprises an unsegmented cephalon, pereon, and pleon. The cephalon has two well-developed black eyes laterally placed. Pereon consists of seven segments (pereonites), with the last two being narrower and pereopods being large. The pleon is smaller than the pereon, with five segments (pleonites) that narrow towards the back. Dark stripes run along the dorsal surface till the uropod and exopods (Fig. 2A). Each female has a marsupium or brood pouch on her ventral surface, containing the eggs and mancae. The pouch showed several black spots, representing the mancae's sensory ocular organs. Pleopods, a pleotelson, and a pair of uropods are seen on the parasite's ventral surface. Uropods have the same lengths and go past the pleotelson line (Fig. 2B). The pouch was sometimes dark grey, and the mancae larvae were freely released from the gravid female (Fig. 2C). Mancae have one pair of large compound eyes, six pairs of legs, and pleopods with setae. The total length of mancae is 1.1-1.3cm with a maximum width of 0.2-0.3cm (Fig. 2A & D).

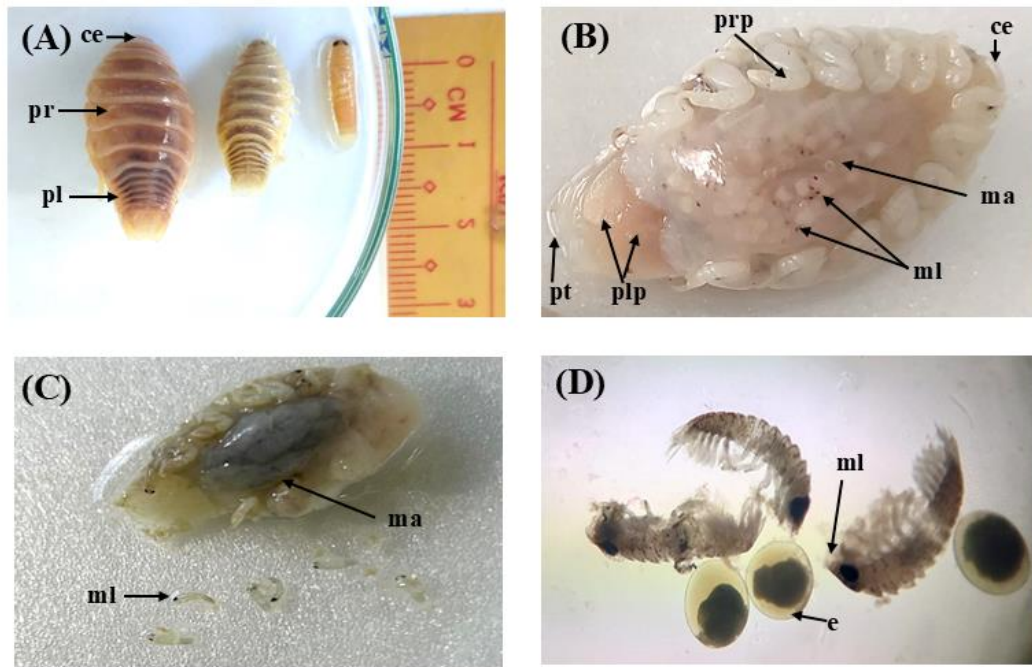


**Fig. 2.** *Livoneca redmanii* from the gills of *Scomberomorus commerson*, Egypt. (A) Dorsal view of female isopod and manca, (B) Ventral view of the gravid female showing immature manca larvae inside the marsupium, (C) Releasing of immature manca larvae from the gravid female, (D) The immature manca larvae and eggs (ce, cephalon; pr, pereon; pl, pleon; prp, pereopods; ma, marsupium; ml, immature manca larvae; plp, pleopods; pt, pleotelson; e, egg)

### *Cathucotyle cathuau* Lebedev, 1968

The body is elongated and tapered at the anterior end. The body length (including haptor) is 6478–12362.2 $\mu$ m (8168.5 $\pm$ 974), while the maximum width is 435.2–1342.2 $\mu$ m (792.2 $\pm$ 138). The haptor is long and tapered posteriorly (Fig. 3A). There is one dorsal vagina and an elongated male copulatory organ with many pectinate spines (Fig. 3B). The testes are numerous. The ovary is horseshoe-shaped and is present in the middle body region and anterior to the testes. Vitellaria are follicular and they occupy the lateral sides of the middle body portion till the haptor (Fig. 3C). The haptor carries 2-4 rows of clamps on either side. The clamp is longer than broad. A precise count is challenging because of the large number of clamps (Fig. 3D). Clamp has a symmetrical structure. The median sclerite is symmetrical, and the basal accessory and lateral sclerites on both sides have a similar width. The clamp carries 6-8 internal ribs (elliptical discs) on each side (Fig. 3E).

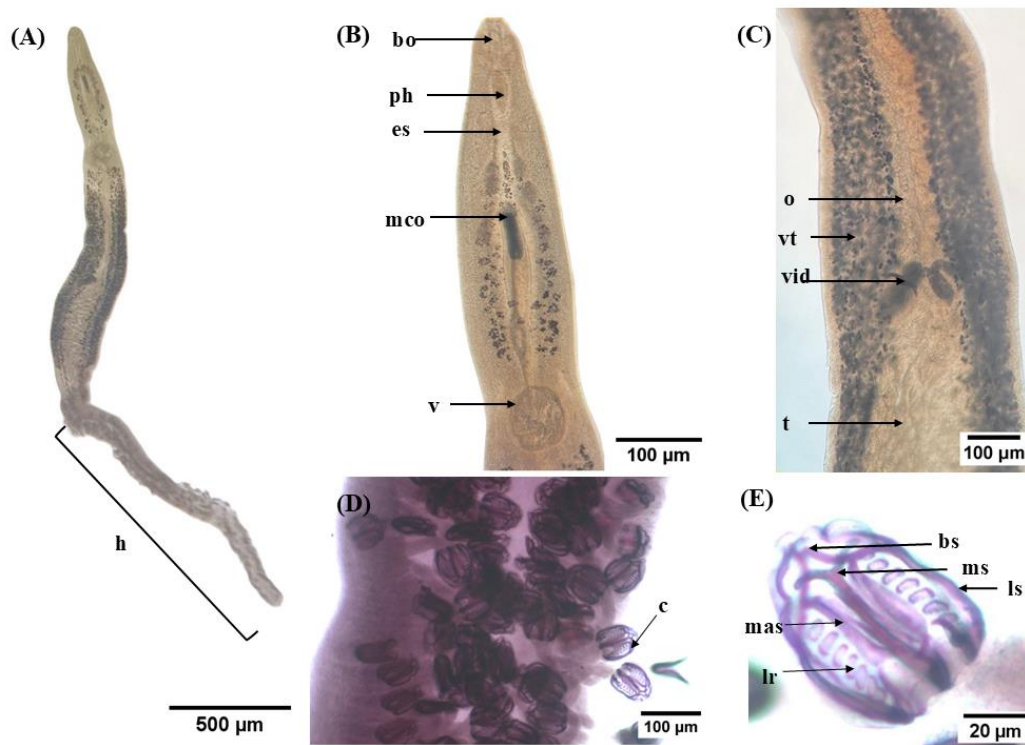


**Fig. 3.** *Cathucotyle cathuauui* from the gills of *Scomberomorus commerson*, Egypt. (A) Unstained whole specimen, (B) The anterior end, (C) The middle part, (D) Haptor, (E) Clamp (h, haptor; bo, buccal opening; ph, pharynx; es, esophagus; mco, male copulatory organ; v, vagina; o, ovary; vt, vitellaria; vid, vitelline duct; t, testes; c, clamps; bs, basal accessory sclerite; ms, median sclerite; mas, median accessory sclerite; ls, lateral sclerite; lr, lateral ribs)

### *Pricea multae* Chauhan, 1945

The total body length is 2783.2-3830.1µm (3359.2±269), and the maximum width is 617.3-848.5µm (699.2±51) at the level of the ovary. The worms have long, smooth bodies that are flattened dorsoventrally and pointed at the anterior end with a bifurcating haptor. The haptor center is linked to the body proper, creating a broad "T" shape (Fig. 4A). Two buccal suckers are present dorsal to the mouth cavity, and the pharynx is posterior to them. There is a single vagina, covered with conical spines (Fig. 4B). The male copulatory organ is clear, with a circle of spines (12-14) with inflated bases and tips that recurve outward (Fig. 4C). The posterior end of the haptor contains one pair of large hamuli with a forked tip. (Fig. 4C). Clamps are numerous and form a single row on each side. The width of clamps exceeds their length (Fig. 4D). Clamps are symmetrical, with 5–7 lateral ribs on either side. The median sclerite is wide, with a broad wing-like median accessory sclerite. External sclerotization is clear (Fig. 4E).

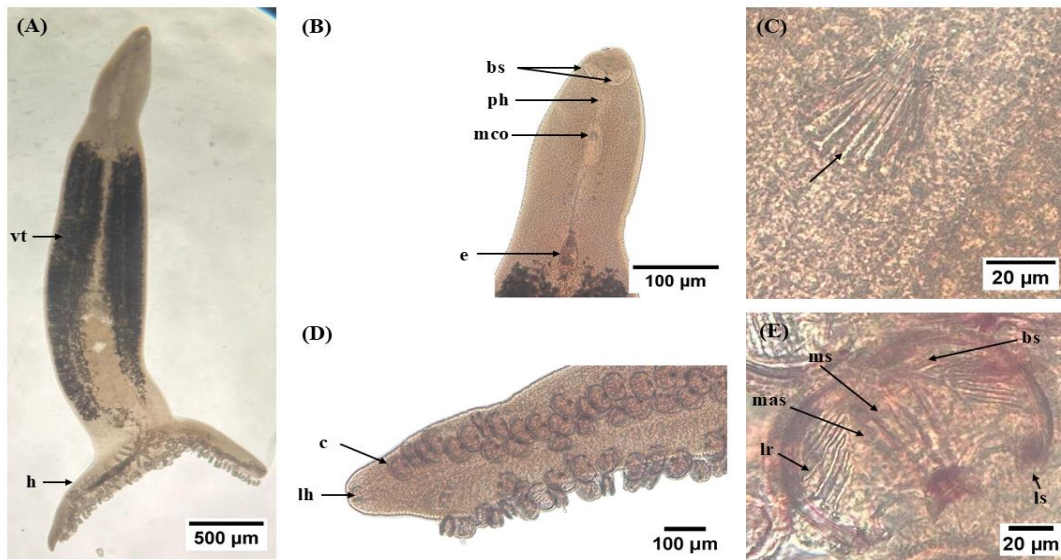


**Fig. 4.** *Pricea multae* from the gills of *Scomberomorus commerson*, Egypt. (A) Unstained whole specimen, (B) The anterior end, (C) Corona of spines of male copulatory organ, (D) Haptor, (E) Clamp (vt, vitellaria; h, haptor; bs, buccal suckers; ph, pharynx; mco, male copulatory organ; e, egg; v, vagina; c, clamps; lh, large hamuli; bs, basal accessory sclerite; ms, median sclerite; mas, median accessory sclerite; ls, lateral sclerite; lr, lateral ribs)

***Pseudothoracocotyla ovalis* (Tripathi, 1956) Yamaguti, 1963**

The body is oval, measuring 3066.6–3911.4 $\mu\text{m}$  ( $3609.1\pm 196$ ) long by 661.5–900.4 $\mu\text{m}$  ( $825\pm 56$ ) wide, broadest at the level of the ovary. Two anterior suckers are present with an oval pharynx behind them. The haptor is asymmetrically connected to the posterior end of the body proper. Vitellarium and gut do not extend into the haptor. The haptor's anterior and posterior ends are devoid of the body proper. Testes are numerous, post-ovarian, and para-ovarian in position (Fig. 5A-C). Clamps (34-40) are organized in two rows and broader than long (Fig. 5D). Clamps resemble suckers (opened). The clamp is divided into two unequal halves that vary in the size of lateral sclerites with 7–10 lateral ribs on either side. The accessory sclerites are absent (Fig. 5E).

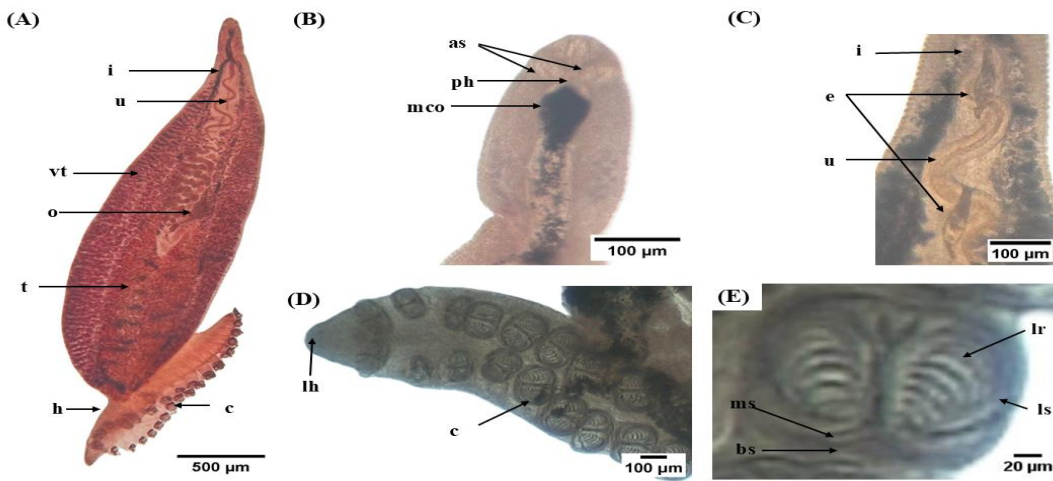


**Fig. 5.** *Pseudothoracocotyla ovalis* from the gills of *Scomberomorus commerson*, Egypt. (A) A whole specimen stained with Semichon's acetocarmine, (B) The anterior end, (C) The intestinal bifurcation part, (D) Haptor, (E) Clamp (i, intestinal ceca; u, uterus; vt, vitellaria; o, ovary; t, testes; h, haptor; as, anterior suckers; ph, pharynx; mco, male copulatory organ; e, egg; c, clamps; lh, large hamuli; bs, basal accessory sclerite; ms, median sclerite; ls, lateral sclerite; lr, lateral ribs)

#### 4. Molecular identification and phylogenetic analysis

The *cox1* gene was amplified from three adult monogenean species (*Cathucotyle cathuauui*, *Pricea multae*, and *Pseudothoracocotyla ovalis*). Gel electrophoresis showed that the amplified *cox1* fragments from all DNA samples were about 600bp, which is in agreement with the expected fragment size. After analyzing and annotating the resulting amplicons, clean sequences were uploaded into GenBank (PQ858431-PQ858433, PV061846).

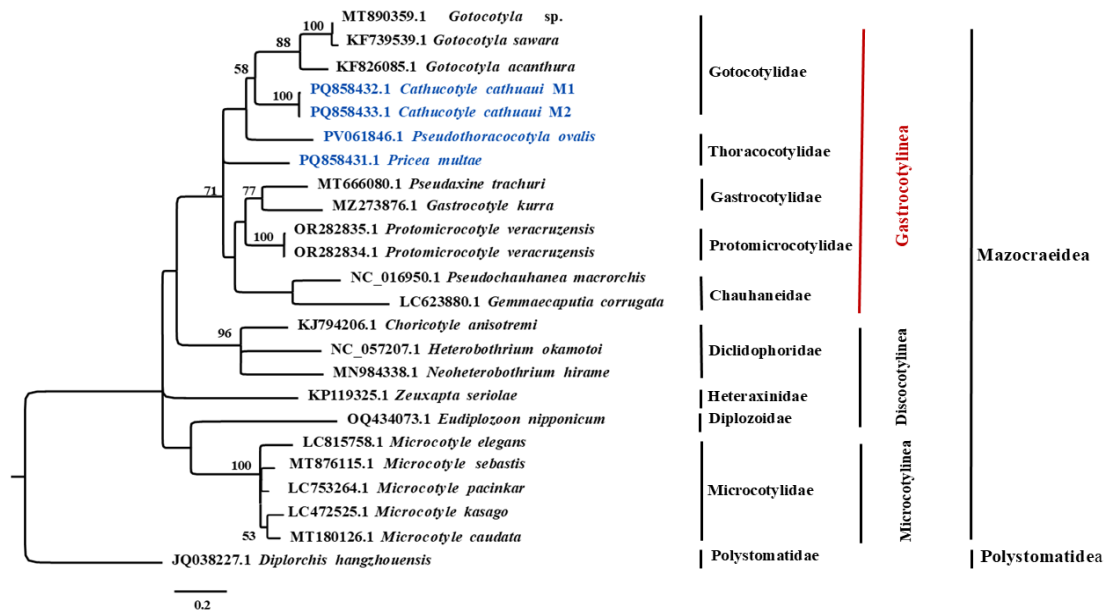
Assessing the nucleotide composition of our sequences demonstrated that the mitochondrial *cox1* gene had an obvious AT bias. The A+T content varied from 62.35 to 68.44%, with the largest amount found in *Pricea multae cox1* sequence. T content had the highest proportion (37.98-44.5%), while C content was the lowest (10.82-15.03%) among the four nucleotide bases.

Table (2) reveals the pairwise distance between 13 *cox1* sequences representing the suborder Gastrocotylea, including the four *cox1* sequences amplified in this study. The *cox1* sequences from the two samples of *Cathucotyle cathuauui* (M1 and M2) were highly similar (1% pairwise distance). These sequences were most closely related to *Gotocotyla acanthura* (KF826085) with 17.1-17.4% pairwise distances, followed by *Gotocotyla* sp. (MT890359, 18.4-18.7%), *Gotocotyla sawara* (KF739539, 18.7-19.3%), and *Protomicrocotyle veracruzensis* (OR282834-OR282835, 18.3-19%). *Pricea multae* was related to *Protomicrocotyle veracruzensis* (OR282834) and *Gotocotyla acanthura*, with 17.3-17.4% pairwise distances, respectively. *Pseudothoracocotyla ovalis cox1* sequence had the lowest genetic distance from *Gotocotyla sawara* (17.4%), followed by *Gotocotyla*

sp. (18.4%), *Protomicrocotyle veracruzensis* (19.6-19.8%), *Pseudaxine trachuri* (MT666080, 20.2%), and *Gotocotyla acanthura* (20.4%).

Fig. (6) shows the ML phylogenetic tree constructed based on 24 polyopisthocotylean *cox1* sequences. Our *cox1* sequences from *Cathucotyle cathuauui*, *Pricea multae*, and *Pseudothoracocotyla ovalis* aggregated in the same clade with members of the suborder Gastrocotylinea (*Gotocotyla* species, *Pseudaxine trachuri*, *Gastrocotyle kurra*, *Protomicrocotyle veracruzensis*, *Pseudochauhanea macrorchis*, and *Gemmaecaputia corrugata*), with 71% bootstrap support. The *cox1* sequences from the two adult samples morphologically identified as *Cathucotyle cathuauui* clustered together in a well-supported branch (100% bootstrap support) and formed a sister group with other members of the Family Gotocotylidae (*Gotocotyla* sp., *G. sawara*, and *G. acanthura*).

The BI phylogenetic tree of the *cox1* sequences had a topology comparable to the ML tree. The suborder Gastrocotylinea, including our sequences from *C. cathuauui*, *P. multae*, and *P. ovalis*, formed a single highly supported clade (probability = 1). *C. cathuauui* M1 and M2 sequences were sister taxa in a well-supported node (probability = 1). Unlike the ML phylogenetic tree, *Gotocotyla* sp., *G. sawara*, and *G. acanthura* were clustered in a separate clade in the BI tree basal to the Gastrocotylinea clade containing our samples but with low support (probability = 0.53). Microcotylinea and Discocotylinea suborders clustered in one clade, supported with 0.99 probability, forming a sister group to the Gastrocotylinea clade (Fig.7).



**Fig. 6.** Maximum likelihood phylogenetic tree based on the mitochondrial *cox1* sequences of polyopisthocotylean monogeneans. Numbers at nodes denote bootstrap value. Nodes with less than 50% support were not annotated. Taxa shown in blue color represent sequences recovered in this study

**Table 2.** Pair-wise genetic distance between the mitochondrial *cox1* sequences of selected Gastrocotylinea monogeneans.

Species	1	2	3	4	5	6	7	8	9	10	11	12	13
GenBank													
1 <i>Cathuotyle cathuaui</i> M1	-												
2 <i>Cathuotyle cathuaui</i> M2	1.0	-											
3 <i>Pricea multae</i>	19.7	19.9	-										
4 <i>Pseudothoracocotyla ovalis</i>	20.7	20.8	21.3	-									
5 <i>Protomicrocotyle veracruzensis</i>	19.0	18.5	17.3	19.8	-								
6 <i>Protomicrocotyle veracruzensis</i>	18.8	18.3	17.8	19.6	0.5	-							
7 <i>Pseudaxine trachuri</i>	19.6	19.9	17.5	20.2	16.6	16.7	-						
8 <i>Gastrocotyle kurra</i>	21.0	21.5	20.7	21.2	17.6	17.9	17.9	-					
9 <i>Gotocotyla</i> sp.	18.4	18.7	20.7	18.4	20.2	20.5	22.0	21.2	-				
10 <i>Gotocotyla acanthura</i>	17.1	17.4	17.4	20.4	20.0	20.4	22.0	21.0	12.6	-			
11 <i>Gotocotyla sawara</i>	18.7	19.3	19.7	17.4	22.0	21.8	23.5	21.9	1.9	12.3	-		
12 <i>Pseudochauhanea macrorchis</i>	23.3	23.5	21.5	21.8	20.7	21.0	20.2	22.5	20.5	19.5	20.1	-	
13 <i>Gemmaecaputia corrugata</i>	26.8	26.9	25.6	27.1	20.6	21.1	23.6	24.1	25.5	26.0	29.1	21.6	-

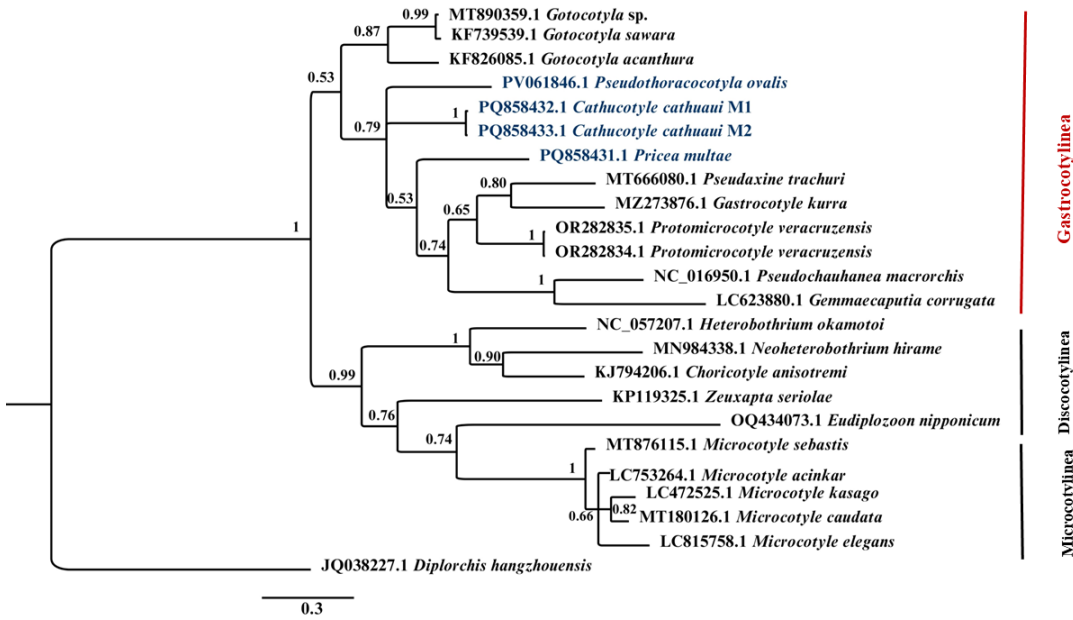


**Fig. 7.** Bayesian inference phylogenetic tree based on the mitochondrial *cox1* sequences of polyopisthocotylean monogeneans. Numbers at nodes denote posterior probabilities (PP). Nodes with PP less than 0.50 were not annotated. Taxa shown in blue color represent sequences recovered in this study

### 5. Biochemical analysis

Table (3) demonstrates the influence of the recorded gill parasites on serum biochemical parameters in *Scomberomorus commerson* fish. The enzyme activity results observed among the three groups, control negative (G1), moderately infested (G2), and heavily infested (G3) fish, showed notable differences. LDH levels increased significantly in G3 and G2 compared to the control group. Similarly, AST and ALT levels were significantly higher in G3 and G2, respectively, compared to G1. ALP activity also followed this trend, with the highest levels recorded in G3, followed by G2, in contrast to the control group. However, The activity of antioxidant enzymes declined, particularly in the heavily infested group (G3). SOD levels were significantly reduced in G3 compared to G1, and CAT activity also decreased notably in both G3 and G2 relative to the control group. Despite these changes, MDA levels, an indicator of lipid peroxidation, remained consistent across all groups. These results collectively highlight the progression of physiological stress and the associated changes in metabolic and antioxidant enzyme activity among the groups.

**Table 3.** The effect of gill parasites on serum biochemical parameters in *Scomberomorus commerson* fish.

Enzyme	G1	G2	G3	Sig,
Lactate dehydrogenase (LDH) U/L	27.82 ± 0.5178 <sup>c</sup>	37.3025 ± 0.325 <sup>b</sup>	47.71 ± 1.107 <sup>a</sup>	**
Aspartate aminotransferase (AST) U/L	96.02 ± 0.636 <sup>c</sup>	114.55 ± 0.791 <sup>b</sup>	118.47 ± 1.105 <sup>a</sup>	**
Alanine aminotransferase (ALT) U/L	26.942 ± 0.225 <sup>b</sup>	27.3525 ± 0.893 <sup>b</sup>	33.755 ± 0.780 <sup>a</sup>	**
Alkaline phosphatase (ALP) U/L	20.825 ± 0.566 <sup>c</sup>	23.9825 ± 0.495 <sup>b</sup>	34.105 ± 0.420 <sup>a</sup>	**
Superoxide dismutase (SOD) U/mL	27.425 ± 0.979 <sup>a</sup>	23.925 ± 0.887 <sup>b</sup>	18.35 ± 0.636 <sup>c</sup>	**
Catalaze (CAT) U/mL	2.8325 ± 0.183 <sup>a</sup>	2.3825 ± 0.208 <sup>a</sup>	1.8225 ± 0.071 <sup>b</sup>	**
Malondialdehyde (MDA) nmol/mL	50.048 ± 0.654 <sup>a</sup>	52.745 ± 0.751 <sup>a</sup>	51.980 ± 0.696 <sup>a</sup>	NS

G1, Control non-infested group (-ve); G2, Moderate infestation (Monogenean infestation); G3, Heavy infestation (mixed infestation with Monogenea and isopods); n=5 in each group, Means within the same row with different superscripts are significantly different ( $P < 0.05$ ); NS, not significant.

## DISCUSSION

The ectoparasites are threatening agents that cause severe economic losses to the fish industry. Because of its ecological and commercial significance, the parasitic isopod crustacea of the family Cymothoidae Leach, 1814, has recently attracted more attention. Isopods are associated with various economically important fishes, resulting in major economic losses for commercial fish species. Adult isopods that are affixed permanently can impede fish growth and reproduction. Pressure atrophy results from attachment and feeding-related injury (Abd EL Maged *et al.*, 2024). Isopods have also been linked to anemia, where they suck the blood of their fish hosts, and the fish become weak due to a lack of oxygen and nutrients. Then, fish become more susceptible to various fatal diseases and secondary infections. Rashed *et al.* (2021) reported that Cymothoid isopods induced atrophy at the connection site and a slight protrusion of the gill cover, in agreement with our clinical and post-mortem results in fish with mixed isopod and

monogenean trematode infestation. Gross lesions observed in gill parasitic infestations in this study included degeneration, atrophy, and a marbled appearance at the attachment site, is consistent with findings from the studies of **Abdel-Mawla and Shalaby (2014)** and **Abd EL Maged et al. (2024)**. Additionally, the occurrence of necrosis and excessive mucus secretions in infested fish aligns with the observations of **El-lamie et al. (2022)**. The presence of pits and tissue damage at the site of isopod attachment agrees with the findings of **Abdallah and Hamouda (2022)**.

In this study, the total prevalence of *Livoneca redmanii* in naturally infected *S. commerson* during the 2024 collection period was 48.7%. This finding is consistent with **Mahmoud et al. (2017)**, who reported a prevalence of 46.5% of *L. redmanii* in various marine fish along Lake Qarun, and with **Helal and Yousef (2018)**, who observed a 46.7% prevalence in *Mugil cephalus* at Lake Qarun. However, the isopod prevalence in this study is higher than the 23% prevalence recorded by **Abdallah and Hamouda (2022)** in the gills of European seabass from the Mediterranean Sea in Kafr Elsheikh Governorate, Egypt, and the 27.1% prevalence reported by **Zayed et al. (2023)** for *Scomberomorus commerson* in Alexandria. The intensity of *L. redmanii* in this study (1-3) is similar to that reported by **Abdallah and Hamouda (2022)** (1-3, with a mean intensity of 1.59). Morphological features observed agree with the descriptions provided by **Mahmoud et al. (2017)**, **Abdallah and Hamouda (2022)** and **Zayed et al. (2023)**. The release of mancae is in line with the findings of **Purivirojkul and Songsuk (2020)**.

In this study, three monogenean species were identified (*Cathucotyle cathuauui*, *Pricea multae*, and *Pseudothoracocotyla ovalis*). These monogenean parasites detected in the branchial cavity co-habituated with isopods (48.7% mixed infestation). According to our knowledge, *C. cathuauui*, and *P. ovalis* have not been recorded in Egypt before, and this is a new locality (Suez Canal) record for these species (**Mansour et al., 2024**). *Cathucotyle cathuauui* is natively distributed throughout the Indo-west Pacific, including South Africa to the Persian Gulf, India, the South China Sea, Indonesia, the Philippines, Australia, and Fiji (**Hayward et al., 1999**). *Pseudothoracocotyla ovalis* is native to the Indo-West Pacific region stretching from South Africa eastward to India, Indonesia, Philippines, Hong Kong, Australia, and Fiji (**Hayward & Rohde, 1999**). Recently, **Rothman et al. (2022)** provided the first report of *C. cathuauui* and *P. ovalis* from the Mediterranean. Our record for these two monogenean species from the Suez Canal suggests the introduction of these parasites from the Indo-West Pacific Ocean to the Mediterranean Sea along with the migration of their host (*S. commerson*) via the Red Sea and Suez Canal.

The total prevalence of monogenean trematodes during the sample collection period was 67.5% which is lower than that recorded by **Rothman et al. (2022)** (100% in *S. commerson* in the Mediterranean Sea) though higher than that reported by **Abd EL Maged et al. (2024)** (38% in Damietta province, Egypt). Monogenean parasite intensity (46–123 parasites/fish) falls within the range reported by **Rothman et al. (2022)** of 15–272 parasites/fish. We recorded *C. cathuauui* in 62.5% in *S. commerson* with an intensity ranging from 12 to 30 parasites/fish. This monogenean parasite was more abundant in the

same fish species examined by **Rothman *et al.* (2022)** (100% prevalence, 10–80 parasites/fish intensity). *P. multae* infested 67.5% of examined fish (the intensity of 29–80 parasites/fish). A lower prevalence was recorded by **Baghdadi *et al.* (2022)** (35%) in the Arabian Gulf, off Jubail, Saudi Arabia, and by **Abd EL Maged *et al.* (2024)** (32%) in the same host. **Rothman *et al.* (2022)** reported *P. multae* with a higher prevalence (100%) in *S. commerson*, however, the intensity (3–84 parasites/fish) was nearly similar to our results. Here, we found *P. ovalis* in 37.5% of examined *S. commerson* (1–13 parasites/fish). **Rothman *et al.* (2022)** found *P. ovalis* in *S. commerson* in the Mediterranean Sea with a higher prevalence (88.9%) and intensity (0–71 parasites/fish). The differing prevalence and intensity of monogeneans can be attributed to variations in collection site and timing.

The morphological characters of *Cathucotyle cathuau* agree with the description of **Hayward *et al.* (1999)** and **Rothman *et al.* (2022)**. *C. cathuau* differed from *Gotocotylole acanthura* previously recorded in Egypt (**El-lamie *et al.*, 2022**) by the symmetrical structure of the clamp (asymmetrical structure in *G. acanthura*), the shape of the internal ribs forming flat and elliptical disc (curved elongated bars in *G. acanthura*), and the clamps are smaller and more numerous than *G. acanthura* (**Hayward *et al.*, 1999**; **Rothman *et al.*, 2022**). The morphological structure of *P. multae* agrees with previous reports by **Rohde and Watson (1996)**, **Baghdadi *et al.* (2022)**, **Rothman *et al.* (2022)** and **Abd EL Maged *et al.* (2024)**. The subfamily Priceinae comprises two genera, *Pricea* and *Mexicotyle* Lebedev, 1984. *P. multae* and *Mexicotyle mexicana* have very similar clamps and male copulatory spines. Meanwhile, the haptor of *M. mexicana* has only one row of clamps and a pair of hamuli without the bifurcated tip (**Rohde & Hayward, 1999**). The morphological description of *Pseudothoracocotylole ovalis* match previous reports of **Hayward and Rohde (1999)** and **Rothman *et al.* (2022)**. *P. ovalis* can be differentiated from *Thoracocotylole* MacCallum, 1913, by the absence of extensive vitellarium and intestine in the haptor (**Hayward & Rohde, 1999**; **Rothman *et al.*, 2022**).

The identification of gastrocotylidans has been confusing, as revealed by the growing list of synonyms that have triggered the revisions of Family Gotocotyloleidae and Thoracocotyloleidae (**Hayward & Rohde, 1999**; **Hayward *et al.*, 1999**; **Rothman *et al.*, 2022**). Combined morphological and molecular methods provide a more efficient tool for identifying monogeneans and clarifying their phylogenetic relationships (**Shi *et al.*, 2014**; **Lewis *et al.*, 2021**; **Baghdadi *et al.*, 2022**; **El-lamie *et al.*, 2022**; **Rothman *et al.*, 2022**). Although mitochondrial DNA is a powerful molecular genetic marker for species-level phylogenetic studies (**Thaenkham *et al.*, 2022**), the *cox1* data of the Family Gotocotyloleidae and Thoracocotyloleidae are lacking. Here, we amplified four *cox1* sequences representing the first mitochondrial DNA data from three monogenean species (*Cathucotyle cathuau*, *Pricea multae*, and *Pseudothoracocotylole ovalis*). There was a clear AT preference in the nucleotide composition of the four amplified sequences, consistent with the AT-rich content in the mitochondrial genes (**Thaenkham *et al.*, 2022**; **Abuzeid *et al.*, 2024a**; **Abuzeid *et al.*, 2024b**). The two *cox1* sequences from samples

morphologically identified as *C. cathuau* were highly homologous with a low nucleotide difference (1%) and were aggregated in the same clade in the phylogenetic tree well-supported with a 100% bootstrap value in the ML phylogeny and a probability value = 1 in the BI phylogeny. These findings suggest that the two sequences belong to the same species (*C. cathuau*), confirming the morphological identification. *C. cathuau* were related to other Gotocotylyds (*Gotocotylya* species) and formed a single clade in the ML phylogeny (58% bootstrap support). This finding concurs with the present classification of the Family Gotocotylyidae and previous phylogenetic studies based on the 28S rRNA (Rothman *et al.*, 2022). Although the BI phylogeny showed that *Gotocotylya* species were basal to all other Gastrocotylinea and did not form a separate node with *C. cathuau*, the probability value did not support this topology. The genetic distance analysis and the ML and BI phylogeny showed that the current classification of the Thoracocotylyidae might not correspond to the phylogenetic relationships between its members (*P. multae* and *P. ovalis*), as suggested by Tambireddy *et al.* (2016) and Rothman *et al.* (2022). The *cox1* sequences of *C. cathuau* (M1 and M2), *P. multae*, and *P. ovalis* were related to taxa representing the suborder Gastrocotylinea. Gastrocotylinea taxa related to our monogenean species represented the Family Gotocotylyidae (*Gotocotylya acanthura*, *Gotocotylya* sp., and *G. sawara*), Protomicrocotylyidae (*Protomicrocotylya veracruzensis*), Gastrocotylyidae (*Pseudaxine trachuri* and *Gastrocotylya kurra*), and Chauhaneidae (*Pseudochauhanea macrorchis* and *Gemmaecaputia corrugata*). The genetic difference between *cox1* sequences of this study and other Gastrocotylinea taxa exceeded 17% nucleotide difference, suggesting that these sequences belong to distinct species. This study reveals the monophyly of the suborder Gastrocotylinea supported with 1 probability and 71% bootstrap in the BI and ML phylogeny, respectively. This result coincides with previous phylogenetic studies (Justine *et al.*, 2013; Tambireddy *et al.*, 2016; Baghdadi *et al.*, 2022; Rothman *et al.*, 2022). ML and BI phylogeny showed that the Gastrocotylinea clade is a sister group to the Discocotylinea and Microcotylinea suborders. In the BI phylogenetic tree, the Discocotylinea and Microcotylinea suborders aggregated together in agreement with the previous 28S rRNA phylogenies (Jovelín & Justine, 2001; Tambireddy *et al.*, 2016; Baghdadi *et al.*, 2022).

The serum biochemical profile is a valuable tool for assessing fish health and detecting disruptions in cellular homeostasis and metabolic balance caused by parasitic infestations (Kumar *et al.*, 2018a). LDH is an enzyme involved in anaerobic metabolism, catalyzing the conversion of pyruvate to lactate. This enzyme is released into the bloodstream or tissues when cells are damaged or under stress, especially in oxygen-deprived conditions (Farhana & Lappin, 2025). This study detected significant LDH increase in heavily (G3) and moderately infested groups (G2) compared to the control non-infested group. Our findings agree with that of Mansell *et al.* (2005) and Kumar *et al.* (2018a), who reported an increase in the serum LDH in the monogenean-infested fish group compared to the non-infested group and observed a decreasing trend of hemoglobin levels with the progression of infestation. Özdemir *et al.* (2016) reported a significant increase in LDH in fish infested with isopods. The reduced capacity of anemic

fish to deliver oxygen to the body may cause anaerobic metabolism and consequent lactate production (**Kumar *et al.*, 2018a**). Elevated lactate levels and increased LDH activity in fish heavily infested with monogenea point to an anemic state and reduced oxygen supply, likely caused by gill dysfunction (**Mansell *et al.*, 2005**), accompanying the gill tissue damage and necrosis. Hypoxia induced by the parasite blocking the respiratory epithelium forces the fish to rely on anaerobic metabolism. Cell membrane disruption leads to the leakage of LDH into the blood and tissues (**Storey & Storey, 2004**). Elevated LDH suggests metabolic stress and indicates that the fish is struggling to meet energy demands (**Farhana & Lappin, 2025**).

Liver enzymes play a specific role in regulating metabolism and are primarily found in the liver. However, AST is also present, though to a lesser extent, in the kidneys and skeletal muscles. ALT and ALP are distributed across various body tissues, particularly in the liver, heart, and skeletal muscles (**Srivastava & Chosdol, 2007**). Elevated liver enzyme activity and higher-than-normal concentrations in the bloodstream often signal tissue or organ damage, leading to the leakage of these enzymes into the blood (**Meyer & Harvey, 1998**). ALP, an enzyme produced by the cells lining the bile ducts of the liver, is a crucial indicator of liver dysfunction and the cell membrane's functional integrity (**Lovatto *et al.*, 2015; Rashidat & Ibitayo, 2018**). The increased activity of ALP is linked to the protective function of organs and tissues responsible for enzyme synthesis, while its decline may be due to a reduction in specific phospholipids necessary for the proper function of this membrane-bound enzyme (**Jiang *et al.*, 2012**). In this study, the activities of AST, ALT, and ALP were significantly higher in the monogenean-infested group compared to the control group. A notable increase in serum AST and ALP levels occurred in heavily and moderately infested groups compared to the non-infested group. ALT levels were significantly elevated in the heavily infested group compared to the control group. This result agrees with that of **Ali and Ansari (2012)**, who reported an upsurge of serum enzyme levels (AST and ALT) in the monogenean-infested common carp. Similarly, elevated activities of AST and ALT in serum occurred in goldfish infested with *Argulus* monogenean parasites (**Kumar *et al.*, 2013**). Fish infested with *Trichodina* sp. and *Cichlidogyrus* sp. ectoparasites displayed a significant and progressive rise in the activity of AST, ALT, and ALP (**Noor El-Deen *et al.*, 2010**). The rise in these enzyme activities indicates liver cell damage or changes in cell membrane permeability, leading to the release of these enzymes into the bloodstream (**Wang *et al.*, 2022**). **El-Deen *et al.* (2010)** attributed the liver enzyme increase to the ongoing irritation and tissue damage caused by severe parasitic infestation. Elevated levels of liver enzymes (AST and ALT) in the serum are a direct consequence of tissue and gill injury and inflammation resulting from the parasitic infestation (**El-Deen *et al.*, 2010**).

Oxidative stress significantly influences the parasite's survival and reproduction. When parasites encounter the host's immune defenses or are treated with antiparasitic agents, they face a rise in reactive oxygen species (ROS) levels, resulting in oxidative stress (**DeMichele *et al.*, 2023**). This oxidative attack can ruin essential biomolecules in the parasite, impairing its capacity to proliferate and evade the host's immune defenses

(Masamba & Kappo, 2021). Parasites have evolved adaptive strategies to combat oxidative stress and to improve their survival by producing antioxidant enzymes and small-molecule antioxidants. These mechanisms neutralize reactive oxygen species and reduce cellular damage, allowing parasites to withstand immune defenses (Rossi & Fasel, 2018). CAT and SOD are key antioxidant enzymes that neutralize ROS. In parasitic infestations, these enzymes may show initial upregulation as the fish attempts to counteract oxidative stress. This trend is followed by enzyme depletion in severe infestations when antioxidant reserves are exhausted (Pawlowska *et al.*, 2023). MDA is a marker of lipid peroxidation (damage to cell membranes). Increased MDA levels indicate oxidative stress caused by the parasite's interference (Gawel *et al.*, 2004). Our results demonstrated that SOD activity significantly decreased in both the heavily (G3) and moderately infested groups (G2) in contrast to the non-infested control group. Similarly, CAT activity was significantly reduced in the heavily infested group (G3) compared to the control. MDA activity showed a non-significant change between the different groups. Our results agree with Furtado *et al.* (2022), who stated that Atlantic salmon with gill infestations exhibit reduced antioxidant potential, likely due to the depletion of antioxidant defenses triggered by infestation and the associated inflammatory response to the parasite. Additionally, previous studies have hypothesized that the parasite may possess an intrinsic mechanism that inhibits the enzymatic production of antioxidants (Marcos-López *et al.*, 2018). During gill parasitic infestation, phagocytic cells increase oxygen consumption, known as an oxygen burst, to eliminate the parasite (Sorci & Faivre, 2009). They also generate superoxide anions and hydrogen peroxide to combat bacterial, viral, and parasitic infestations (Maldonado *et al.*, 2020). Parasitic infestations lead to an imbalance between ROS and antioxidant defenses, resulting in oxidative stress that damages proteins, lipids, and DNA in the gill tissues (Pawlowska *et al.*, 2023).

## CONCLUSION

This study highlights the prevalence and impact of gill parasites on *Scomberomorus commerson* in the Suez Canal, Egypt. Four parasitic species, comprising Cymothoid isopods (*Livoneca redmanii*) and monogenean trematodes (*Cathucotyle cathuau*, *Pricea multae*, and *Pseudothoracocotyla ovalis*), were identified, with *P. multae* being the most prevalent and intense. Notably, this is the first record of *C. cathuau* and *P. ovalis* in Egypt. The mitochondrial *cox1* gene was first amplified from these three monogenean species and used to reveal their phylogenetic relationship. Biochemical and pathological analyses revealed significant alterations in infested fish. These findings underscore the detrimental impact of gill parasites on fish health, emphasizing the need for effective control measures to mitigate their effects. Furthermore, the study establishes the mt *cox1* gene as a reliable marker for monogenean identification, which could aid in better monitoring and controlling parasitic infestations in aquaculture.

## REFERENCES

- Abd EL Maged, R., R; Rasheed, N.; Ibrahim, I.; Saad, H.M.; Batiha, G.E.-S. and Abou Zaid, A.A.** (2024). New insights on the effects of monogenean gill parasites on naturally infested *Scoberomorus commerson*: host response, electron microscopy, and histopathological studies. *Damanhour J. Vet. Sci.* , 11(1): 20-25. <https://doi.org/10.21608/DJVS.2023.248877.1125>.
- Abdallah, E.S.H. and Hamouda, A.H.** (2022). *Livoneca redmanii* Leach, 1818 (Cymothoidae) a parasitic isopod infesting the gills of the European seabass, *Dicentrarchus labrax* (Linnaeus, 1758): morphological and molecular characterization study. *BMC Vet. Res.*, 18(1): 330. <https://doi.org/10.1186/s12917-022-03405-2>.
- Abdel-Mawla, I.H. and Shalaby, I.N.** (2014). Some studies on monogeniasis and its relation to some heavy metals levels in *Scoberomorus commerson* from Red sea. *Abbassa Int. J. Aqua*, 7(1): 225-248.
- Abuzeid, A.M.; Hefni, M.M.; El-Gayar, A.K.; Huang, Y. and Li, G.** (2024a). Prevalence and identification of cyathocotylid trematodes infecting African catfish in Egypt. *Parasitol. Res.*, 123(10): 1-16. <https://doi.org/10.1007/s00436-024-08375-y>.
- Abuzeid, A.M.; Hefni, M.M.; Huang, Y.; Zhuang, T. and Li, G.** (2024b). Phylogenetic relationship of *Prohemistomum vivax* to other trematodes based on the internal transcribed spacer region and mitochondrial genes. *Parasitol. Res.*, 123(1): 113. <https://doi.org/10.1007/s00436-024-08126-z>.
- Aebi, H.** (1984). [13] Catalase in vitro. In: "Methods in Enzymology". Academic Press, pp. 121-126.
- Ali, H. and Ansari, K.** (2012). Comparison of haematological and biochemical indices in healthy and monogenean infected common carp, *Cyprinus carpio*. *Ann. Biol. Res.*, 3(4): 1843-1846.
- Aneesh, P.-T.; Sudha, K.; Helna, A.K.; Anilkumar, G. and Trilles, J.-P.** (2014). Multiple parasitic crustacean infestation on belonid fish *Strongylura strongylura*. *ZooKeys*, (457): 339. <https://doi.org/10.3897/zookeys.457.6817>.
- Assane, I.M.; Prada-Mejia, K.D.; Gallani, S.U.; Weiser, N.F.; Valladão, G.M.R. and Pilarski, F.** (2022). *Enterogyrus* spp. (Monogenea: Ancyrocephalinae) and *Aeromonas jandaei* co-infection associated with high mortality following transport stress in cultured Nile tilapia. *Transbound. Emerg. Dis.*, 69(4): e276-e287. <https://doi.org/10.1111/tbed.14295>.
- Baghdadi, H.B.; Al-Salem, A.A.M.; Ibrahim, M.M.; Younes, A.M.; Aboelenin, S.M. and Bayoumy, E.M.** (2022). Morphomolecular identification and considerations of the infestation site adaptations of *Pricea multae* (Thoracocotylidae: Priceinae) from *Scomberomorus commerson*, off Arabian Gulf, Saudi Arabia. *Rev. Bras. Parasitol. Vet.*, 31(3): e007122. <https://doi.org/10.1590/S1984-29612022041>.

- Bird, R.P. and Draper, H.H.** (1984). [35] Comparative studies on different methods of malonaldehyde determination. In: "Methods in Enzymology". Academic Press, pp. 299-305.
- Brusca, R.C.** (1981). A monograph on the Isopoda Cymothoidae (Crustacea) of the eastern Pacific. Zool. J. Linn. Soc., 73(2): 117-199. <https://doi.org/10.1111/j.1096-3642.1981.tb01592.x>.
- Cabaud, P.G. and Wroblewski, F.** (1958). Colorimetric measurement of lactic dehydrogenase activity of body fluids. Am J Clin Pathol, 30(3): 234-236. <https://doi.org/10.1093/ajcp/30.3.234>.
- Cantanhêde, S.M.; Sodr -Campos, V.C.; Pereira, D.P.; Medeiros, A.M.; Fortes-Carvalho-Neta, R.N.; Tchaicka, L. and Silva-Santos, D.M.** (2018). Parasitism in gills of *Centropomus undecimalis* (Pisces, Centropomidae) from a protected area in S o Lu s, Maranh o, Brazil. Lat. Am. J. Aquat. Res., 46(2): 377-382. <https://doi.org/10.3856/vol46-issue1-fulltext-13>.
- Çenesiz, S.** (2020). The role of oxidant and antioxidant parameters in the infectious diseases: A systematic literature review. Kafkas Univ. Vet. Fak. Derg., 26(6). <https://doi.org/10.9775/kvfd.2020.24618>
- Conroy, D.A. and Herman, R.L.** (1970). Textbook of fish diseases, ed. TFH Publications, West Sylvania.
- DeMichele, E.; Sosnowski, O.; Buret, A.G. and Allain, T.** (2023). Regulatory functions of hypoxia in host–parasite interactions: a focus on enteric, tissue, and blood protozoa. Microorganisms, 11(6): 1598. <https://doi.org/10.3390/microorganisms11061598>.
- Di Natale, A.; El-Haweet, A.E.A.; Abouelmagd, N.; Lahoud, I. and Bariche, M.** (2020). Fisheries of the narrow-barred Spanish mackerel (*Scomberomorus commerson*, Lac p de, 1800) in the southern and eastern Mediterranean Sea and relevance of this species to ICCAT. Collect. Vol. Sci. Pap. ICCAT, 77(9): 85-99.
- Di Natale, A.; Srour, A.; Hattour, A.; Keskin, Ç.; Idrissi, M. and Orsi Relini, L.** (2009). Regional study on small tunas in the Mediterranean including the Black Sea. Studies and Reviews., ed. FAO, Rome.
- Dickson, K.B. and Zhou, J.** (2020). Role of reactive oxygen species and iron in host defense against infection. Front. Biosci. (Landmark Ed), 25(8): 1600-1616. <https://doi.org/10.2741/4869>.
- El-lamie, M.M.; Ali, A.; Abouelhassan, E.M.; Ismail, A. and El-Sheshtawy, H.M.** (2022). Molecular phylogeny and histopathological studies of *Gotocotyula secundus* (Monogenea: Polyopisthocotylea) isolated from Narrow-barred Spanish mackerel, *Scomberomorus commerson* in Suez Governorate, Egypt. Egypt. J. Aquat. Biol. Fish., 26(4). <https://doi.org/10.21608/ejabf.2022.253695>.
- Estiarte, M.; Peuelas, J.; Sardans, J.; Emmett, B.; Sowerby, A.; Beier, C.; Schmidt, I.; Tietema, A.; Van Meeteren, M. and Kovacs-Lang, E.** (2007). Root-surface phosphatase activity in shrublands across a European gradient: effects of warming. J. Environ. Biol., 29(1): 25.

- Farhana, A. and Lappin, S.L.** (2025). Biochemistry, lactate dehydrogenase. In: "StatPearls". StatPearls Publishing LLC., Treasure Island (FL),
- Furtado, F.; Breiland, M.W.; Strand, D.; Timmerhaus, G.; Carletto, D.; Pedersen, L.-F.; Afonso, F. and Lazado, C.C.** (2022). Regulation of the molecular repertoires of oxidative stress response in the gills and olfactory organ of Atlantic salmon following infection and treatment of the parasite *Neoparameoba perurans*. *Fish & Shellfish Immunol.*, 130: 612-623. <https://doi.org/10.1016/j.fsi.2022.09.040>.
- Gawel, S.; Wardas, M.; Niedworok, E. and Wardas, P.** (2004). Dialdehyd malonowy (MDA) jako wskaźnik procesów peroksydacji lipidów w organizmie [Malondialdehyde (MDA) as a lipid peroxidation marker]. *Wiad Lek*, 57(9-10): 453-455.
- Hayward, C.** (2005). Monogenea Polyopisthocotylea (ectoparasitic flukes). In: "Marine Parasitology". Rohde, K. (ed). Csiro publishing, Collingwood, pp. 55-63.
- Hayward, C.J. and Rohde, K.** (1999). Revision of the monogenean subfamily Thoracocotylineae Price, 1936 (Polyopisthocotylea: Thoracocotylidae), with the description of a new species of the genus *Pseudothoracocotyla* Yamaguti, 1963. *Syst. Parasitol.*, 44(3): 157-169. <https://doi.org/10.1023/a:1006236713378>.
- Hayward, C.J.; Rohde, K. and Hayward, C.J.** (1999). Revision of the monogenean family Gotocotylidae (Polyopisthocotylea). *Invertebr. Syst.*, 13(3): 425-460. <https://doi.org/10.1071/IT98003>.
- Helal, A.M. and Yousef, O.E.** (2018). Infestation study of *Livoneca redmanii* (Isopoda, Cymothoidae) on *Mugil cephalus* in Lake Qarun, Egypt. *Egypt. Acad. J. Biol. Sci., B. Zool.*, 10(1): 1-17. <https://doi.org/10.21608/eajbsz.2018.13425>.
- Huang, X.-J.; Choi, Y.-K.; Im, H.-S.; Yarimaga, O.; Yoon, E. and Kim, H.-S.** (2006). Aspartate aminotransferase (AST/GOT) and alanine aminotransferase (ALT/GPT) detection techniques. *Sensors*, 6(7): 756-782. <https://doi.org/10.3390/s6070756>.
- Jiang, H.; Yang, H.; Kong, X.; Wang, S.; Liu, D. and Shi, S.** (2012). Response of acid and alkaline phosphatase activities to copper exposure and recovery in freshwater fish *Carassius auratus gibelio* var. *Life Sci.*, 9(3): 233-245.
- Jovelin, R. and Justine, J.-L.** (2001). Phylogenetic relationships within the polyopisthocotylean monogeneans (Platyhelminthes) inferred from partial 28S rDNA sequences. *Int. J. Parasitol.*, 31(4): 393-401. [https://doi.org/10.1016/S0020-7519\(01\)00114-X](https://doi.org/10.1016/S0020-7519(01)00114-X).
- Justine, J.-L.; Rahmouni, C.; Gey, D.; Schoelinck, C. and Hoberg, E.P.** (2013). The monogenean which lost its clamps. *PLOS ONE*, 8(11): e79155. <https://doi.org/10.1371/journal.pone.0079155>.
- Katoh, K.; Rozewicki, J. and Yamada, K.D.** (2017). MAFFT online service: multiple sequence alignment, interactive sequence choice and visualization. *Brief. Bioinform.*, 20(4): 1160-1166. <https://doi.org/10.1093/bib/bbx108>.
- Kumar, S.; Raman, R.; Kumar, K.; Pandey, P.; Kumar, N.; Mallesh, B.; Mohanty, S. and Kumar, A.** (2013). Effect of azadirachtin on haematological and

- biochemical parameters of *Argulus*-infested goldfish *Carassius auratus* (Linn. 1758). *Fish Physiol. Biochem.*, 39(4): 733-747. <https://doi.org/10.1007/s10695-012-9736-8>.
- Kumar, S.; Raman, R.P.; Prasad, K.P.; Srivastava, P.; Kumar, S. and Rajendran, K.** (2018a). Effects on haematological and serum biochemical parameters of *Pangasianodon hypophthalmus* to an experimental infection of *Thaparocleidus* sp. (Monogenea: Dactylogyridae). *Exp. Parasitol.*, 188: 1-7. <https://doi.org/10.1016/j.exppara.2018.02.007>.
- Kumar, S.; Stecher, G.; Li, M.; Knyaz, C. and Tamura, K.** (2018b). MEGA X: molecular evolutionary genetics analysis across computing platforms. *Mol. Biol. Evol.*, 35(6): 1547. <https://doi.org/10.1093/molbev/msy096>.
- Lewisch, E.; Führer, H.P.; Shahi-Barogh, B.; Harl, J. and El-Matbouli, M.** (2021). Emergence of *Discocotyle sagittata* (Monogenea: Polyopisthocotylea) in rainbow trout (*Oncorhynchus mykiss*) and brown trout (*Salmo trutta*) in an Austrian aquarium. *J. Fish Dis.*, 44(10): 1643-1646. <https://doi.org/10.1111/jfd.13470>.
- Lia, R.P.; Zizzo, N.; Tinelli, A.; Lionetti, A.; Cantacessi, C. and Otranto, D.** (2007). Mass mortality in wild greater amberjack (*Seriola dumerili*) infected by *Zeuxapta seriolae* (Monogenea: Heteraxinidae) in the Jonian Sea. *Bull. Eur. Assoc. Fish Pathol.*, 27(3): 108.
- Lovatto, N.d.M.; Goulart, F.R.; de Freitas, S.T.; Mombach, P.I.; Loureiro, B.B.; Bender, A.B.B.; Boligon, A.A.; Radünz Neto, J. and da Silva, L.P.** (2015). Nutritional evaluation of phosphorylated pumpkin seed (*Cucurbita moschata*) protein concentrate in silver catfish *Rhamdia quelen* (Quoy and Gaimard, 1824). *Fish Physiol. Biochem.*, 41(6): 1557-1567. <https://doi.org/10.1007/s10695-015-0107-0>.
- Mahmoud, N.E.; Fahmy, M. and Abuowarda, M.** (2017). An investigation of Cymothoid isopod invasion in lake Qarun fishes with preliminary trial for biological control. *Int. J. Chemtech Res.*, 10(2): 409-416.
- Maldonado, E.; Rojas, D.A.; Morales, S.; Miralles, V. and Solari, A.** (2020). Dual and opposite roles of reactive oxygen species (ROS) in Chagas disease: beneficial on the pathogen and harmful on the host. *Oxid. Med. Cell. Longev.*, 2020(1): 8867701. <https://doi.org/10.1155/2020/8867701>.
- Mansell, B.; Powell, M.; Ernst, I. and Nowak, B.F.** (2005). Effects of the gill monogenean *Zeuxapta seriolae* (Meserve, 1938) and treatment with hydrogen peroxide on pathophysiology of kingfish, *Seriola lalandi* Valenciennes, 1833. *J. Fish Dis.*, 28(5): 253-262. <https://doi.org/10.1111/j.1365-2761.2005.00625.x>.
- Mansour, A.; Sarabeev, V. and Balbuena, J.A.** (2024). Checklist of monogeneans from Egyptian marine fishes, including some newly collected species. *Syst. Parasitol.*, 101(3): 28. <https://doi.org/10.1007/s11230-024-10150-7>.
- Marcos-López, M.; Espinosa, C.R.; Rodger, H.; O'connor, I.; MacCarthy, E. and Esteban, M.** (2018). Oxidative stress is associated with late-stage amoebic gill

- disease in farmed Atlantic salmon (*Salmo salar* L.). *J. Fish Dis.*, 41: 383-387. <https://doi.org/10.1111/jfd.12699>.
- Masamba, P. and Kappo, A.P.** (2021). Immunological and biochemical interplay between cytokines, oxidative stress and schistosomiasis. *Int. J. Mol. Sci.*, 22(13): 7216. <https://doi.org/10.3390/ijms22137216>.
- Meyer, D.J. and Harvey, J.** (1998). Evaluation of hepatobiliary system and skeletal muscle and lipid disorders. In: "Veterinary Laboratory Medicine: Interpretation and Diagnosis". pp. 157–187.
- Mozhdeganloo, Z. and Heidarpour, M.** (2014). Oxidative stress in the gill tissues of goldfishes (*Carassius auratus*) parasitized by *Dactylogyrus* spp. *J. Parasit. Dis.*, 38(3): 269-272. <https://doi.org/10.1007/s12639-013-0239-z>.
- Nishikimi, M.; Appaji, N. and Yagi, K.** (1972). The occurrence of superoxide anion in the reaction of reduced phenazine methosulfate and molecular oxygen. *Biochem. Biophys. Res. Commun.*, 46(2): 849-854. [https://doi.org/10.1016/s0006-291x\(72\)80218-3](https://doi.org/10.1016/s0006-291x(72)80218-3).
- Noor El-Deen, A.; Mona, M.; Mohamed, A. and Omima, A.** (2010). Comparative studies on the impact of humic acid and formalin on ectoparasitic infestation in Nile tilapia *Oreochromis niloticus*. *Nat. Sci.*, 8(2): 121-125.
- Özdemir, G.; Çelik, E.Ş.; Yılmaz, S.; Gürkan, M. and Kaya, H.** (2016). Histopathology and blood parameters of bogue fish (*Boops boops*, Linnaeus 1758) parasitized by *Ceratothoa oestroides* (Isopoda: Cymothoidae). *Turk. J. Fish. Aquat. Sci.*, 16(3): 579-590. [https://doi.org/10.4194/1303-2712-v16\\_3\\_28](https://doi.org/10.4194/1303-2712-v16_3_28).
- Pawłowska, M.; Mila-Kierzenkowska, C.; Szczegieliński, J. and Woźniak, A.** (2023). Oxidative stress in parasitic diseases—Reactive oxygen species as mediators of interactions between the host and the parasites. *Antioxidants*, 13(1): 38. <https://doi.org/10.3390/antiox13010038>.
- Purivirojkul, W. and Songsuk, A.** (2020). New records of fish parasitic isopods (Crustacea: Isopoda) from the Gulf of Thailand. *Animals*, 10(12): 2298. <https://doi.org/10.3390/ani10122298>.
- Rashed, M.; Fadel, S.E. and Elnady, A.M.** (2021). Effect of Isopoda on the health status of gilthead seabream (*Sparus aurata*). *Egypt. J. Anim. Health* 1(1): 34-43. <https://doi.org/10.21608/ejah.2021.133607>.
- Rashidat, T. and Ibitayo, A.** (2018). Growth response, nutrient utilization, biochemical and hematological parameters of juvenile African catfish (*Clarias gariepinus*) fed diet supplemented with *Gongronema latifolia* (Benth) extract. *Egypt. J. Aquat. Biol. Fish.*, 22(4): 167-179. <https://doi.org/10.21608/ejabf.2018.16562>.
- Rohde, K. and Hayward, C.J.** (1999). Revision of the monogenean subfamily Priceinae Chauhan, 1953 (Polyopisthocotylea: Thoracocotylidae). *Syst. Parasitol.*, 44(3): 171-182. <https://doi.org/10.1023/a:1006288730216>.
- Rohde, K. and Watson, N.A.** (1996). Ultrastructure of the buccal complex of *Pricea multae* (Monogenea: Polyopisthocotylea, Gastrocotylidae). *Folia Parasitol.*, 43(2): 117-132.

- Rossi, M. and Fasel, N. (2018). How to master the host immune system? *Leishmania* parasites have the solutions! *Int. Immunol.*, 30(3): 103-111. <https://doi.org/10.1093/intimm/dxx075>.
- Rothman, S.B.; Diamant, A. and Goren, M. (2022). Under the radar: co-introduced monogeneans (Polyopisthocotylea: Gastrocotylina) of the invasive fish *Scomberomorus commerson* in the Mediterranean Sea. *Parasitol. Res.*, 121(8): 2275-2293. <https://doi.org/10.1007/s00436-022-07560-1>.
- Shi, S.F.; Li, M.; Yan, S.; Wang, M.; Yang, C.P.; Lun, Z.R.; Brown, C.L. and Yang, T.B. (2014). Phylogeography and demographic history of *Gotocotyla sawara* (Monogenea: Gotocotylidae) on Japanese Spanish mackerel (*Scomberomorus niphonius*) along the Coast of China. *J. Parasitol.*, 100(1): 85-92. <https://doi.org/10.1645/13-235.1>.
- Silva, M.; Freitas, M. and Orge, M. (1997). Co-infection by monogenetic trematodes of the genus *Microcotyle* V. Beneden & Hesse 1863, *Lamellodiscus ignoratus* Palombi, 1943, the protozoan *Trichodina* sp. Ehrenberg, 1838 and the presence of epitheliocystis, *Vibrio alginolyticus* and *V. vulnificus* in cultured seabream (*Sparus aurata* L.) in Portugal. *Bull. Eur. Ass. Fish Pathol.*, 17(2): 40-42.
- Sorci, G. and Faivre, B. (2009). Inflammation and oxidative stress in vertebrate host-parasite systems. *Philos. Trans. R. Soc. B: Biol. Sci.*, 364(1513): 71-83. <https://doi.org/10.1098/rstb.2008.0151>.
- Srivastava, T. and Chosdol, K. (2007). Clinical enzymology and its applications. *Clinical Bio-chem*, 4: 3-4.
- Storey, K.B. and Storey, J.M. (2004). Oxygen limitation and metabolic rate depression. In: "Functional metabolism: regulation and adaptation". Storey, K.B. (ed). Wiley, Ontario, pp. 415-442.
- Svobodová, Z. and Vykusová, B. (1991). Diagnostics, prevention and therapy of fish diseases and intoxications: manual for international training course on fresh-water fish diseases and intoxications: diagnostics, prophylaxis and therapy. Institute of Fish Culture and Hydrobiology, Vodnany.
- Szewczyk-Golec, K.; Pawłowska, M.; Wesółowski, R.; Wróblewski, M. and Mila-Kierzenkowska, C. (2021). Oxidative stress as a possible target in the treatment of toxoplasmosis: perspectives and ambiguities. *Int. J. Mol. Sci.*, 22(11): 5705. <https://doi.org/10.3390/ijms22115705>.
- Tambireddy, N.; Gayatri, T.; Gireesh-Babu, P. and Pavan-Kumar, A. (2016). Molecular characterization and phylogeny of some mazocraeidean monogeneans from carangid fish. *Acta Parasitol.*, 61(2): 360-368. <https://doi.org/10.1515/ap-2016-0047>.
- Tesfay, S.; Teferi, M.; Dejenie, T.; Abay, T. and Hiluf, G. (2024). A survey of ecto and endoparasites of Nile tilapia, *Oreochromis niloticus* (Linnaeus, 1758) fingerlings in Midmar reservoir, Adwa, northern Ethiopia. *J. Appl. Anim. Res.*, 52(1): 2310158. <https://doi.org/10.1080/09712119.2024.2310158>.

- Tessema, W.** (2020). Review on parasites of fish and their public health importance. *ARC J. Anim. Vet. Sci*, 6: 23-27. <https://doi.org/10.20431/2455-2518.0602004>.
- Thaenkham, U.; Chaisiri, K. and Hui En Chan, A.** (2022). Molecular genetic markers: general use in parasitic helminth researches. In: "Molecular Systematics of Parasitic Helminths". Thaenkham, U.; Chaisiri, K. & Hui En Chan, A. (eds). Springer, Singapore, pp. 161-181.
- Thai, V.N.; Dehbandi, R.; Fakhri, Y.; Sarafraz, M.; Nematollahi, A.; Dehghani, S.S.; Gholizadeh, A. and Mousavi Khaneghah, A.** (2021). Potentially toxic elements (PTEs) in the fillet of narrow-barred Spanish mackerel (*Scomberomorus commerson*): a global systematic review, meta-analysis and risk assessment. *Biol. Trace Elem. Res.*, 199(9): 3497-3509. <https://doi.org/10.1007/s12011-020-02476-2>.
- Wang, J.; Hussain, R.; Ghaffar, A.; Afzal, G.; Saad, A.Q.; Ahmad, N.; Nazir, U.; Ahmad, H.I.; Hussain, T. and Khan, A.** (2022). Clinicohematological, mutagenic, and oxidative stress induced by pendimethalin in freshwater fish bighead carp (*Hypophthalmichthys nobilis*). *Oxid. Med. Cell. Longev.*, 2022(1): 2093822. <https://doi.org/10.1155/2022/2093822>.
- Yıldırım, P.; Kan, Ş.; Güçlü, S.S.; Özmen, Ö.; Özdamar, A.; Bahrioğlu, E. and Kubilay, A.** (2024). Bacterial and parasitic co-infection in *Carassius gibelio* Bloch, 1782 caught in the Onaç reservoir, Türkiye. *J. Hell. Vet. Med. Soc.*, 75(2): 7315-7324. <https://doi.org/10.12681/jhvms.34180>.
- Zayed, O.E.; Hellal, A.M.; Zeina, A.F. and Tayel, S.I.** (2023). Prevalence of parasitic isopods (Cymothoidae and Gnathiidae) on *Actinopterygii* fishes from the Alexandria coast off the Mediterranean Sea, Egypt. *Egypt. J. Aquat. Biol. Fish.*, 27(4). <https://doi.org/10.21608/ejabf.2023.313131>.
- Zhang, J.; Wu, X.; Xie, M. and Li, A.** (2012). The complete mitochondrial genome of *Pseudochauhanea macrorchis* (Monogenea: Chauhaneidae) revealed a highly repetitive region and a gene rearrangement hot spot in Polyopisthocotylea. *Mol. Biol. Rep.*, 39(8): 8115-8125. <https://doi.org/10.1007/s11033-012-1659-z>.